



**HAL**  
open science

# Microwave-driven generation and group delay control of optical pulses from an ultra-dilute atomic ensemble

J K Saaswath, K N Pradosh, K V Adwaith, Barry C Sanders, Fabien Bretenaker, Andal Narayanan

► **To cite this version:**

J K Saaswath, K N Pradosh, K V Adwaith, Barry C Sanders, Fabien Bretenaker, et al.. Microwave-driven generation and group delay control of optical pulses from an ultra-dilute atomic ensemble. Optics Express, 2021, 29 (11), pp.15940. 10.1364/oe.424110 . hal-03223332

**HAL Id: hal-03223332**

**<https://hal.science/hal-03223332>**

Submitted on 10 May 2021

**HAL** is a multi-disciplinary open access archive for the deposit and dissemination of scientific research documents, whether they are published or not. The documents may come from teaching and research institutions in France or abroad, or from public or private research centers.

L'archive ouverte pluridisciplinaire **HAL**, est destinée au dépôt et à la diffusion de documents scientifiques de niveau recherche, publiés ou non, émanant des établissements d'enseignement et de recherche français ou étrangers, des laboratoires publics ou privés.

# Microwave-driven generation and group delay control of optical pulses from an ultra-dilute atomic ensemble

J. K. SAASWATH,<sup>1</sup> K. N. PRADOSH,<sup>1</sup> K. V. ADWAITH,<sup>1</sup>  BARRY C. SANDERS,<sup>1,2</sup>  FABIEN BRETENAKER,<sup>1,3</sup>  AND ANDAL NARAYANAN<sup>1,\*</sup>

<sup>1</sup>Raman Research Institute, Sir C V Raman Avenue, Sadashivnagar, Bangalore 560080, India

<sup>2</sup>Institute for Quantum Science and Technology, University of Calgary, Alberta, T2N 1N4, Canada

<sup>3</sup>Université Paris-Saclay, CNRS, ENS Paris-Saclay, CentraleSupélec, LuMIn, 91190 Gif-sur-Yvette, France

\*andal@rri.res.in

**Abstract:** A cyclic atomic level scheme interacting with an optical and a microwave field is proposed for the generation and group-delay control of few-photon optical pulses. Our analysis exploits a hybrid second order-nonlinearity under conditions of electromagnetically induced transparency to generate an optical pulse. The generated pulse can be delayed or advanced through microwave intensity control of the absolute phase of the second-order-nonlinearity. Importantly, this handle on group delay of the generated pulse is number density-independent. Our scheme is thus ideally suited for the generation and control of few-photon optical pulses using ultra-dilute atomic samples. Our results will enable microscopic atomic interface systems that serve as controllable delay channels for both classical and quantum signal processing.

© 2021 Optical Society of America under the terms of the [OSA Open Access Publishing Agreement](#)

## 1. Introduction

Generating few-photon and single-photon [1–4] pulses-on-demand is an important resource for many applications in quantum enabled technologies. Several practically realized quantum key distribution protocols use attenuated laser pulses [5,6] whereas quantum repeaters and quantum computing modules use single-photon pulses-on-demand [2–4,7]. Such few-photon on-demand sources are traditionally implemented through controllable semiconductor sources such as quantum dots and color centers in crystals [8].

Dilute atomic sample-based controllable generation, storage and transmission of single-photon pulses has been experimentally realized [9,10]. Such atom-based generation schemes relies on the Electromagnetically Induced Transparency (EIT) effect and is important for practical realization of quantum networks. A large number of EIT-based systems have been studied for controlling the group delay of pulses. In these systems control of propagation dynamics of an input pulse as subluminal [11–15] and superluminal [16–19] propagation have been both experimentally and theoretically investigated. In addition there are studies that provide a knob to change the propagation of light from subluminal to superluminal [18–25], giving control for continuous tunability of group delay. Observation of nonlinear generation of subluminal and superluminal pulses using EIT-based schemes in atomic vapours [26–28] has been experimentally investigated too. These studies are of particular importance in realising optical delay lines [29], optical coherence tomography [30] and pulse-jitter corrections [27].

In the above mentioned studies of EIT-based generation and control of photon pulses done so far, efficiency of the process is directly proportional to number density and spatial extent of the sample. This scaling limits the prospect of integration of these systems with chip-based integrated circuit devices, which are being increasingly used as a platform for realising scalable quantum technological architectures [31].

We propose a mechanism to control generation and group delay of a few-photon optical pulse that is independent of density and spatial extent of the generating sample. Generation of a few-photon optical probe pulse is made possible using a hybrid second order-nonlinearity induced through a cyclic closed three-level scheme in a dilute atomic system. As the probe pulse is generated by a sum-frequency process between pump field photons, it can be made on-demand by tailoring the time when one of the pump fields, either the optical field or the microwave field, is switched on.

We show that group delay of the optical pulse can be controlled by the intensity of the pump microwave field. This tunable control has the characteristics of subluminal and superluminal propagation of light but arises from a different physical effect. The intensity of the pump field alters the absolute phase for different frequencies present within the generated optical pulse resulting in changes in the group delay. Most significant of all, this control is shown to be *number density-independent* and hence can be achieved with few atoms resulting in few-photons per pulse. For experimentally feasible parameters, we show that a group delay of the order of 1  $\mu\text{s}$  can be achieved with an ultra-dilute density of  $10^6 \text{ cm}^{-3}$ . At such densities we show that the generated optical pulse has approximately a mean photon number of one. Sample lengths as small as 100  $\mu\text{m}$  has been shown to introduce changes in group delay paving the way for integration of such system with chip based photonic architectures.

## 2. Deriving linear and second-order susceptibilities for the probe field in a cyclic scheme

We consider a generic cyclic and closed  $\Lambda$  atomic level scheme illustrated in Fig. 1. Such a scheme could be realized using the hyperfine levels of  $^{85}\text{Rb}$  around the D1 transition. This generic scheme consists of an excited state  $|1\rangle$ , a metastable state  $|2\rangle$  and a ground state  $|3\rangle$ . The resonance frequencies of the transitions in Fig. 1 are  $\omega_{13}, \omega_{12}$  and  $\omega_{23}$  respectively. The probe field is weak compared to the coupling and microwave fields. The three fields together with the three transitions form a closed  $\Lambda$  system, referred to as a  $\Delta$  system [32] hereafter. The electric field representation of the continuous-wave (CW) probe, coupling and the magnetic field representation of the CW microwave are given by

$$\vec{E}_p(\tau) = \vec{e}_p \mathcal{E}_p \cos(\omega_p \tau), \vec{E}_c(\tau) = \vec{e}_c \mathcal{E}_c \cos(\omega_c \tau), \vec{B}_\mu(\tau) = \vec{e}_\mu \mathcal{E}_\mu \cos(\omega_\mu \tau), \quad (1)$$

where  $\tau = t - z/c$ , with their initial phases taken to be zero.  $\vec{e}_i, \mathcal{E}_i$  and  $\omega_i$  for  $i \in \{p, c, \mu\}$  are the polarization, amplitude and frequency labels of the respective fields.

To understand linear and second-order processes involving the  $|1\rangle \leftrightarrow |3\rangle$  transition in our  $\Delta$  system and their effect on the probe field, linear electric susceptibility  $\chi_p^{(1)}(\omega_p)$  and hybrid second-order susceptibility  $\chi_p^{(2)}(\omega_c, \omega_\mu)$  for the probe field are calculated. The hybrid  $\chi_p^{(2)}(\omega_c, \omega_\mu)$  corresponds to generation of the probe field by a combination of electric-and magnetic-dipole transitions mediated by coupling and microwave electromagnetic fields, respectively.

The susceptibilities are calculated analytically by solving the master equation for the atomic density operator ( $\rho$ ) to first order in probe amplitude. The density-matrix equations in the rotating frame are

$$\begin{aligned} \dot{\sigma}_{11} &= -2(\gamma_{13} + \gamma_{12})\sigma_{11} + i\Omega_c \sigma_{21} + i\Omega_p e^{-i\Delta_c \tau} \sigma_{31} - i\Omega_c^* \sigma_{12} - i\Omega_p^* e^{i\Delta_c \tau} \sigma_{13}, \\ \dot{\sigma}_{22} &= -2\gamma_{23} \sigma_{22} + 2\gamma_{12} \sigma_{11} + i\Omega_c^* \sigma_{12} + i\Omega_\mu \sigma_{32} - i\Omega_c \sigma_{21} - i\Omega_\mu^* \sigma_{23}, \\ \dot{\sigma}_{12} &= -(\gamma_{13} + \gamma_{12} + \gamma_{23} - i\Delta_c) \sigma_{12} + i\Omega_p e^{-i\Delta_c \tau} \sigma_{32} + i\Omega_c \sigma_{22} - i\Omega_c \sigma_{11} - i\Omega_\mu^* \sigma_{13}, \\ \dot{\sigma}_{13} &= -(\gamma_{13} + \gamma_{12} - i(\Delta_c + \Delta_\mu)) \sigma_{13} + i\Omega_c \sigma_{23} - i\Omega_\mu \sigma_{12} + i\Omega_p e^{-i\Delta_c \tau} (1 - \sigma_{22} - \sigma_{11}) \\ &\quad - i\Omega_p e^{-i\Delta_c \tau} \sigma_{11}, \\ \dot{\sigma}_{23} &= -(\gamma_{23} - i\Delta_\mu) \sigma_{23} - i\Omega_p e^{-i\Delta_c \tau} \sigma_{21} + i\Omega_c^* \sigma_{13} - i\Omega_\mu \sigma_{22} + i\Omega_\mu (1 - \sigma_{22} - \sigma_{11}), \end{aligned} \quad (2)$$

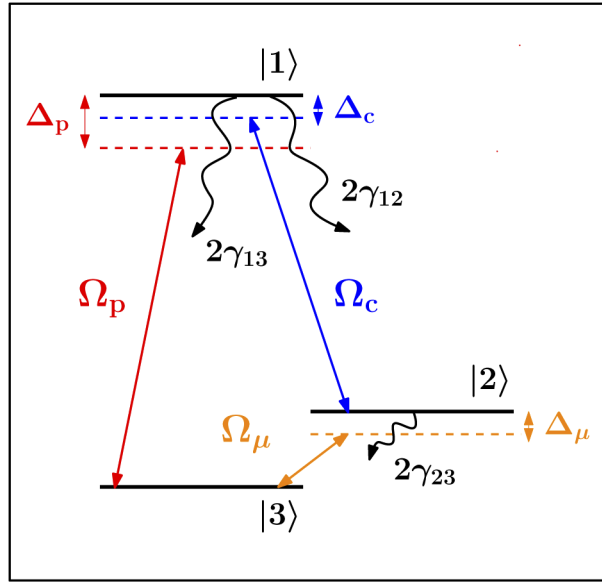


**Fig. 1.** Schematic diagram of  $\Delta$  atomic system. Electric dipole allowed transitions  $|1\rangle \leftrightarrow |3\rangle$  and  $|1\rangle \leftrightarrow |2\rangle$  are coupled by two optical fields called probe ( $\Omega_p$ ) and coupling ( $\Omega_c$ ), respectively. The magnetic dipole allowed transition  $|2\rangle \leftrightarrow |3\rangle$  is connected by a microwave field ( $\Omega_\mu$ ).

where the off-diagonal elements represent atomic coherences of the system; particularly,  $\sigma_{13}$  is our quantity of interest for calculating pertinent susceptibilities. Rotated  $\sigma$  matrix elements are related to the original matrix elements  $\rho$  by the unitary transformation

$$\rho_{12} = \sigma_{12}e^{-i\omega_c\tau}, \quad \rho_{13} = \sigma_{13}e^{-i(\omega_c+\omega_\mu)\tau}, \quad \rho_{23} = \sigma_{23}e^{-i\omega_\mu\tau}. \quad (3)$$

In Eqs. (2),  $2\gamma_{13}$  is the decay rate for  $|1\rangle \rightarrow |3\rangle$ ,  $2\gamma_{12}$  is the decay rate for  $|1\rangle \rightarrow |2\rangle$  and  $2\gamma_{23}$  is the decay rate for  $|2\rangle \rightarrow |3\rangle$ . The Rabi frequencies of the probe, coupling and microwave fields are defined as

$$2\Omega_p = \frac{\vec{e}_p \cdot \vec{d}_{13}\mathcal{E}_p}{\hbar}, \quad 2\Omega_c = \frac{\vec{e}_c \cdot \vec{d}_{12}\mathcal{E}_c}{\hbar}, \quad 2\Omega_\mu = \frac{\vec{e}_\mu \cdot \vec{\mu}_{23}\mathcal{E}_\mu}{\hbar}, \quad (4)$$

where  $\vec{d}_{13}$ ,  $\vec{d}_{12}$  are electric-dipole matrix elements for the transitions  $|1\rangle \leftrightarrow |3\rangle$ ,  $|1\rangle \leftrightarrow |2\rangle$  respectively and  $\vec{\mu}_{23}$  is the magnetic-dipole matrix element for the  $|2\rangle \leftrightarrow |3\rangle$  transition. The quantities

$$\Delta_p = \omega_p - \omega_{13}, \quad \Delta_c = \omega_c - \omega_{12}, \quad \Delta_\mu = \omega_\mu - \omega_{23}, \quad (5)$$

are detunings of probe, coupling and microwave fields from their respective transitions. Three-photon detuning of all three fields is defined as

$$\Delta_t = \Delta_p - \Delta_c - \Delta_\mu. \quad (6)$$

Scalar polarization of the atoms, induced by electromagnetic fields to first order in probe amplitude, is

$$P(\tau) \approx \varepsilon_0\mathcal{E}_p(\chi_p^{(1)}(\omega_p)e^{-i\omega_p\tau} + \text{c.c.})/2 + \varepsilon_0\mathcal{E}_c\mathcal{E}_\mu(\chi_p^{(2)}(\omega_c, \omega_\mu)e^{-i(\omega_c+\omega_\mu)\tau} + \text{c.c.})/4, \quad (7)$$

and, in terms of the density-matrix elements using Eq. (3), is

$$P(\tau) = \mathcal{N}(d_{13}\sigma_{13}e^{-i(\omega_c+\omega_\mu)\tau} + d_{12}\sigma_{12}e^{-i\omega_c\tau} + \text{c.c.}), \quad (8)$$

where  $\mathcal{N}$  is the number density of atoms. The susceptibilities of probes  $\chi_p^{(1)}$ ,  $\chi_p^{(2)}$  are obtained by calculating  $\sigma_{13}$  to first order in probe amplitude [20]. Towards this, we expand density-matrix elements  $\sigma_{jk}$  of (2) as

$$\sigma_{jk} = \sigma_{jk}^{(0)}\Omega_c\Omega_\mu + \sigma_{jk}^{(1)}\Omega_\mu e^{-i\Delta_c\tau} + \sigma_{jk}^{(2)}\Omega_\mu^* e^{i\Delta_c\tau} \quad (9)$$

$(j, k \in \{1, 2, 3\}).$

The perturbative expansion (9) is substituted in Eqs. (2), and we neglect terms of order  $\Omega_p^2$  as  $\Omega_p \ll \Omega_\mu$  &  $\Omega_c$ . The unknowns  $\sigma_{jk}^{(0)}$ ,  $\sigma_{jk}^{(1)}$ ,  $\sigma_{jk}^{(2)}$  are found by solving the resulting linear equations. Required susceptibilities are obtained by substituting Eq. (9) for  $\sigma_{13}$  in Eq. (8) and comparing it with Eq. (7), giving us

$$\chi_p^{(2)}(\omega_c + \omega_\mu, \omega_c, \omega_\mu) = \left( \frac{4Nd_{13}d_{12}\mu_{23}}{\varepsilon_0\hbar^2} \right) \sigma_{13}^{(0)}(\Omega_c, \Omega_\mu, \Delta_c, \Delta_\mu), \quad (10)$$

$$\chi_p^{(1)}(\omega_p, \omega_p) = \left( \frac{2Nd_{13}^2}{\varepsilon_0\hbar} \right) \sigma_{13}^{(1)}(\Omega_c, \Omega_\mu, \Delta_c, \Delta_\mu, \Delta_p). \quad (11)$$

In the succeeding section,  $\chi_p^{(1)}$  and  $\chi_p^{(2)}$  are used to study the group delay and temporal profile of the generated probe pulse.

### 3. Pulsed probe-field generation and manipulation of group delay

In this section we study the  $\Delta$  system without the input probe field and investigate the effect of various parameters on group delay of a generated probe pulse, generated through the hybrid second order-nonlinearity  $\chi_p^{(2)}$ . Towards this we use a modified  $\Delta$  scheme given in Fig. 2.

With the help of susceptibility expressions given in Eqs. (10) and (11), we calculate the temporal profile for a generated probe pulse. To ensure pulse-probe generation, we employ an input Gaussian pulsed microwave field,

$$\Omega_\mu(z=0, \Delta_\mu) = (2\Omega_\mu^0 \sqrt{2\pi}/\delta) e^{-\Delta_\mu^2/2\delta^2} \quad (12)$$

driving  $|2\rangle \leftrightarrow |3\rangle$ , where  $2\Omega_\mu^0$  and  $\delta$  are the amplitude and spectral width of the envelope, respectively. The coupling field in Fig. 2 is the same as the one in Fig. 1, a CW with  $\Delta_c = 0$ . The input fields are taken to be propagating along the positive  $z$ -direction. The vapour cell has length  $l$  and extends from  $z = 0$  to  $l$ , and the input fields are defined at the entrance to the cell at  $z = 0$ .

Due to  $\chi_p^{(2)}$  the pulsed microwave field combines with the CW optical coupling field to give rise to a pulsed probe field through a sum-frequency generation process. By conservation of energy, the generated probe detuning ( $\Delta_p$ ) will be equal to the microwave detuning, i.e.,  $\Delta_p = \Delta_\mu$ . Such a generation was theoretically studied [33] and already experimentally observed by us [34].

The input microwave pulse and the CW optical coupling fields are undepleted pump fields. The magnitudes of the propagation vectors of the coupling, microwave and probe fields inside

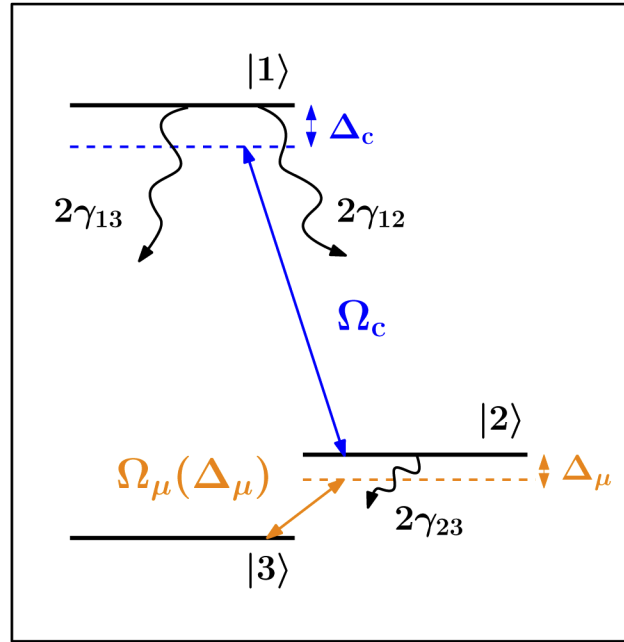


**Fig. 2.** Pulsed microwave field  $\Omega_\mu(\Delta_\mu)$  and a CW coupling field  $\Omega_c$  is used to observe pulsed probe generation through the nonlinear susceptibility  $\chi_p^{(2)}$ .

the vapour cell are

$$k_c^2 = \frac{\omega_{12}^2(1 + \chi_c^{(1)})}{c^2}, \quad k_\mu^2 = \frac{(\omega_{23} + \Delta_\mu)^2(1 + \chi_\mu^{(1)})}{c^2}, \quad (13)$$

$$k_p^2 = \frac{(\omega_{13} + \Delta_p)^2(1 + \chi_p^{(1)})}{c^2}, \quad (14)$$

where  $\chi_c^{(1)}, \chi_\mu^{(1)}$  are the linear susceptibilities of the coupling and microwave fields. The wave-vector mismatch of the generated probe field is defined as  $\Delta k = (k_c + k_\mu) - k_p$ . We assume a length  $l$  for the cell such that  $\Delta kl \ll 1$  over the bandwidth of the microwave pulse. For brevity the arguments of the following functions are suppressed :  $\Omega_\mu(\Delta_p) = \Omega_\mu$ ,  $k_p(\Delta_p) = k_p$  and  $\chi_p^{(2)}(\Delta_p) = |\chi_p^{(2)}|e^{i\phi^{(2)}}$ . Under the assumptions stated above, the temporal envelope of the generated probe pulse at  $z = l$  in the slowly varying amplitude approximation [35] is

$$\Omega_p^g(l, t) = \int_{-\infty}^{\infty} \frac{i(\omega_{13} + \Delta_p)^2 l \Omega_\mu \Omega_c |\chi_p^{(2)}| e^{i\phi^{(2)}} e^{i(k_p l - (\omega_{13} + \Delta_p)t)}}{K c^2 k_p} d\Delta_p, \quad (15)$$

where  $K = 2\pi\mu_{23}d_{12}/\hbar d_{13}$ . For simplicity, the microwave pulse bandwidth is assumed to be small enough such that only the effect of central frequency is considered for estimation of  $\chi_p^{(1)}$ . As can be seen from Eq. (15), the dynamics of the generated probe pulse profile depends on the complex ( $\mathbb{C}$ ) quantities  $\chi_p^{(1)}$  and  $\chi_p^{(2)}$ . We study in-detail the effects of linear and non-linear susceptibility on the amplitude and group delay of the generated probe pulse.

The amplitude of the generated probe pulse depends on  $|\chi_p^{(2)}|$  and the imaginary part of  $\chi_p^{(1)}$  ( $\chi_{ip}^{(1)}$ ). Under two-photon resonance between the generated probe pulse and the coupling pulse our system satisfies all the conditions necessary for showing EIT effect as seen in Fig. 3. At

two-photon resonance, ( $\Delta_p = 0$ ) the typical value of  $\chi_{Ip}^{(1)}$  is around  $10^{-7}$ . To make sure that the generated probe pulse suffers negligible absorption due to  $\chi_{Ip}^{(1)}$ , the generated probe bandwidth is chosen to be within the EIT window through appropriate choices of  $\delta$  and  $\Omega_c$  values. Henceforth we assume that absorption of the generated pulse due to linear susceptibility is negligible. We therefore drop terms relating to  $\chi_{Ip}^{(1)}$  from Eq. (15).

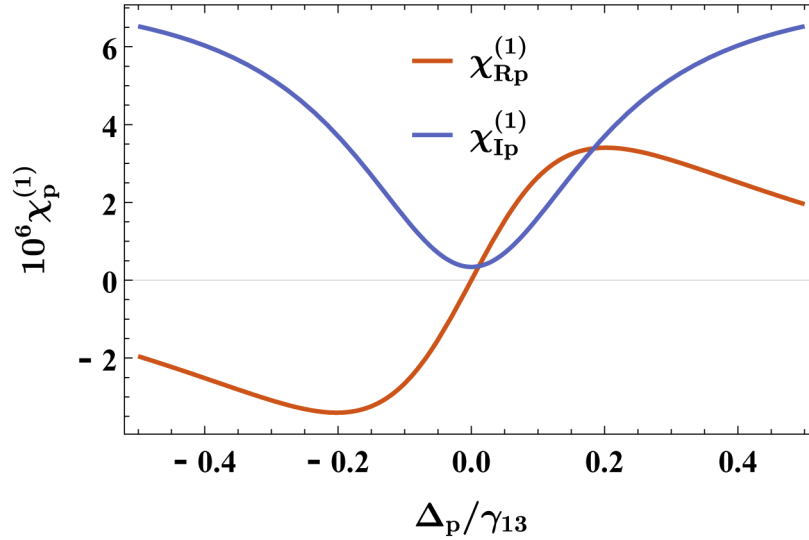


**Fig. 3.** Real and imaginary parts of the linear susceptibility as a function of generated probe detuning, for  $\Omega_c = 0.4\gamma_{13}$ ,  $\Omega_\mu^0 = 0.004\gamma_{13}$ ,  $\gamma_{23} = 0.004\gamma_{13}$ ,  $\gamma_{13} = 5\pi \times 10^6$  rad/s and  $\mathcal{N} = 10^8$  cm $^{-3}$ .

Group delay of the generated probe with respect to a reference pulse is defined as the time difference in peak arrival time of the generated probe pulse and the reference pulse, both calculated at the end of the vapour cell. The peak here is defined as the peak of the generated optical pulse with maximum amplitude. The reference is a Gaussian pulse traversing the same length in vacuum given by

$$\Omega_r(l, t) = \frac{1}{2\pi} \int_{-\infty}^{\infty} (\Omega_r^0 \sqrt{2\pi}/\sigma) e^{-\Delta_p^2/2\sigma^2} e^{i(\omega_{13} + \Delta_p)(l/c - t)} d\Delta_p, \quad (16)$$

where  $\Omega_r^0$  and  $\sigma$  are the amplitude and spectral width of the reference respectively.

This group delay depends on two qualitatively different spectral phases acquired by the generated probe as seen in Eq. (15). The first spectral phase is the traditional propagation phase  $\phi^{(1)} = k_p l$ . Using Eq. (14) we derive an expression for  $\phi^{(1)}$

$$\phi^{(1)} \approx \frac{(\omega_{13} + \Delta_p)(1 + \chi_{Rp}^{(1)}/2)l}{c}, \quad (17)$$

where  $\chi_{Rp}^{(1)}$  is the real part of  $\chi_p^{(1)}$ . The second one is the generation phase, the initial phase probe pulse acquires during the generation process. This is defined as

$$\phi^{(2)} = \arg(\chi_p^{(2)}), \quad (18)$$

which is the phase of complex  $\chi_p^{(2)}$ .

Our main results presented below are due to the effect of  $\phi^{(2)}$  on the group delay of the generated probe pulse. To calculate the group delay to first order, we perform a Taylor expansion of the phases  $\phi^{(1)}$  and  $\phi^{(2)}$  around  $\Delta_p = 0$ ,

$$\phi^{(k)} \approx \phi^{(k)} \Big|_{\Delta_p=0} + \frac{\partial \phi^{(k)}}{\partial \Delta_p} \Big|_{\Delta_p=0} \Delta_p \quad (k \in \{1, 2\}). \quad (19)$$

We identify the pertinent temporal quantities in the above expansion and classify them as

$$t^{(1)} = \frac{\partial \phi^{(1)}}{\partial \Delta_p} \Big|_{\Delta_p=0} = \frac{n_g l}{c}, \quad (20)$$

$$n_g = 1 + (1/2) \chi_{\text{Rp}}^{(1)} \Big|_{\Delta_p=0} + (1/2) \frac{\partial \chi_{\text{Rp}}^{(1)}}{\partial \Delta_p} \Big|_{\Delta_p=0} \omega_{13}, \quad (21)$$

$$t^{(2)} = \frac{\partial \phi^{(2)}}{\partial \Delta_p} \Big|_{\Delta_p=0}. \quad (22)$$

Substituting Eqs. (17)–(22) in Eq. (15) we calculate the total group delay of the generated probe pulse with respect to the reference pulse. This is done by comparing the complex phases in Eqs. (15) and (16). Thus the total group delay ( $T_g$ ) of the generated probe pulse with respect to the reference is given by

$$T_g = t^{(1)} + t^{(2)} - l/c. \quad (23)$$

In the above expression  $t^{(1)}$  is the traditional group delay associated with  $c/n_g$ , the group velocity of the pulse. On the other hand,  $t^{(2)}$  is the group delay associated with the change of the generated probe initial phase with changing probe frequency. In the subsequent paragraphs we analyse each of the  $t^{(1)}$  and  $t^{(2)}$  contributions to the total group delay for different number densities of atoms.

There have been numerous studies on the group delay  $t^{(1)}$  due to changes in group velocity of an input pulse traversing a coherently prepared atomic medium [11–25]. Some of these studies focused on developing a knob for changing the group velocity from subluminal to superluminal resulting in delay or advancement respectively of the peak of an input pulse [18–25]. These changes in group delay are due to the real part of linear susceptibility and are number density-dependent as seen from Eq. (11).

To explicitly illustrate this density dependence, we show in Fig. 4 the group delay due to  $\chi_{\text{Rp}}^{(1)}$  as a function of  $\Omega_\mu^0$  for two different number densities. For a density value of  $\mathcal{N} = 10^8 \text{ cm}^{-3}$  we see that the group delay changes from positive to negative as a function of  $\Omega_\mu^0$  because of subluminal to superluminal change in group velocity. However by reducing the density by two orders to  $\mathcal{N} = 10^6 \text{ cm}^{-3}$  we observe not only that the group delay remains practically constant with changing  $\Omega_\mu^0$ , but also that its value is close to zero indicating that the group velocity of the pulse numerically approximates its value in vacuum. Thus we note that any knob to change the value and sign of the group velocity of a pulse which is density-dependent is unlikely to work for low-density samples.

In contrast to the heavy dependence of  $t^{(1)} - l/c$  on  $\mathcal{N}$  and  $l$ , the group delay due to  $t^{(2)}$  is independent of  $\mathcal{N}l$ , representing a density-independent group delay due to nonlinear generation. Mathematically  $\mathcal{N}$  is a prefactor to both the real and imaginary part of  $\chi_p^{(2)}$  (Eq. (10)) and, since  $\phi^{(2)}$  is the argument of  $\chi_p^{(2)}$ , it is independent of  $\mathcal{N}$  leading to  $t^{(2)}$  also being  $\mathcal{N}$  independent. The physical origin of  $\phi^{(2)}$  being independent of  $\mathcal{N}$  is that this is the phase associated with the generated probe field by the atoms during the generation process. In the absence of atom-atom interaction this generation phase is independent of the number density.



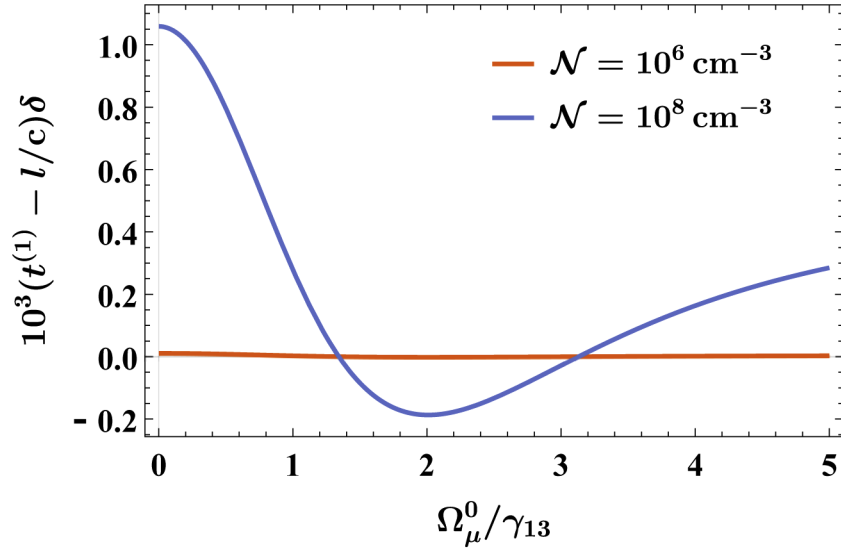


**Fig. 4.** Group delay, due to the real part of linear susceptibility, as a function of microwave amplitude, for  $\Omega_c = 3.2\gamma_{13}$ ,  $\delta = 0.3 \times 10^6$  Hz,  $\gamma_{13} = 5\pi \times 10^6$  rad/s and  $l = 1$  cm.

For the purpose of generation of few-photons we henceforth will work with low-density samples. We show in our subsequent analysis how we can effect both an advancement and a delay in the peak of a few-photon pulse through  $t^{(2)}$ . The knob we use to change the sign of  $t^{(2)}$  is the intensity of the microwave pulse.

We fix the input optical pump field ( $\Omega_c$ ) to be  $0.4\gamma_{13}$  with its beam diameter taken to be  $1 \text{ mm}^2$  and the spectral width of the input microwave pulse to be  $\delta = 0.3 \times 10^6$  Hz. The total energy in the generated pulse is given by

$$E = (b\hbar^2/d_{13}^2) \int_{-\infty}^{\infty} \varepsilon_0 c |\Omega_p^g(l, t)|^2 dt, \quad (24)$$

where  $b$  is the beam diameter. The number of photons in the pulse is estimated by dividing the total energy ( $E$ ) by the energy of the central frequency photon ( $\hbar\omega_{13}$ ). By this procedure we find that a few-photon pulse is generated at the output for  $N = 10^6 \text{ cm}^{-3}$  and  $l = 1$  cm. For these  $N$  and  $l$  values, the group-delay contribution from  $(t^{(1)} - l/c)$  through linear susceptibility can be safely ignored as can be seen in Fig. 4.

This leads to minimising the effect of  $\chi_{Rp}^{(1)}$  in Eq. (15), leading to the final generated probe profile as

$$\Omega_p^g(l, t) = \int_{-\infty}^{\infty} \frac{i(\omega_{13} + \Delta_p) l \Omega_c \Omega_\mu |\chi_p^{(2)}| e^{i\phi^{(2)}} e^{i(\omega_{13} + \Delta_p)(l/c - t)}}{Kc} d\Delta_p, \quad (25)$$

and its group delay with respect to the reference

$$T_g = t^{(2)}. \quad (26)$$

Now the group delay of the generated few-photon pulse with respect to the reference pulse originates entirely from the generation phase  $\phi^{(2)}$  and not due to any propagation effect.

As shown in Fig. 5 the atoms generate different frequencies of probe with different initial phases and this phase profile clearly depends on  $\Omega_\mu^0$ . We can see that the slope around the  $\Delta_p = 0$  value changes sign for two different  $\Omega_\mu^0$  values. As  $t^{(2)}$  is the slope of  $\phi^{(2)}$  at  $\Delta_p = 0$ , it is clear from Fig. 5 that one can use  $\Omega_\mu^0$  as a handle to delay or advance the generated probe pulse.

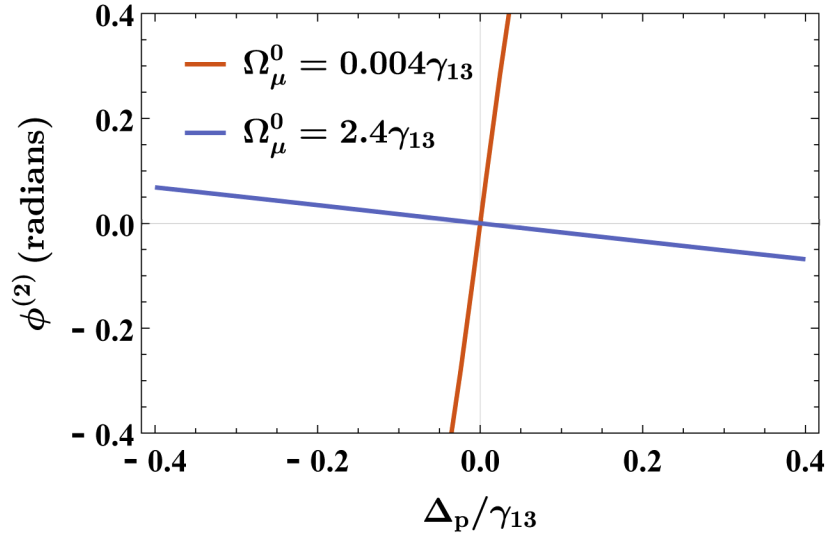


**Fig. 5.** Generation phase as a function of the generated probe detuning, for  $\Omega_c = 0.4\gamma_{13}$ ,  $N = 10^6 \text{ cm}^{-3}$  and  $\gamma_{13} = 5\pi \times 10^6 \text{ rad/s}$ .

We will quantitatively estimate the group delay of the generated probe pulse through changes in pump field intensities. We plot in Fig. 6,  $t^{(2)}$  as a function of  $\Omega_\mu^0$ . This plot shows that  $\Omega_\mu^0$  can be used as a knob for continuous tunability of  $t^{(2)}$  resulting in delay or advancement in peak of the pulse. Such a continuous tunability is also achievable through changes in  $\Omega_c$ . The temporal profile of the generated probe pulse is obtained by numerical integration of Eq. (25) and is shown in Figs. 7 and 8. These plots show a pulse delay of  $0.5 \mu\text{s}$  and a pulse advancement of  $0.3 \mu\text{s}$  respectively, for a change of  $\Omega_\mu^0 = 0.004\gamma_{13}$  to  $\Omega_\mu^0 = 2.4\gamma_{13}$  at  $N = 10^6 \text{ cm}^{-3}$ . To observe the same order of delay or advancement in an input probe pulse through propagation effects, one requires a number density of the order  $10^{11} \text{ cm}^{-3}$ . Thus, by manipulating the generated phase profile even with very dilute samples of atoms, comparable changes in group delay can be achieved.

The temporal shape of the generated pulse is governed by  $|\chi_p^{(2)}|$  as seen in Eq. (25). Our calculations show that the delayed and advanced probe pulse temporal width (standard deviation) in Figs. 7 and 8 is contracted by 79% and 91% respectively, with respect to the input pulsed microwave. As can be seen, the higher value of  $\Omega_\mu^0$  required for advancement of the generated pulse shown in Fig. 8 results in increased temporal distortion of the generated pulse. For higher microwave intensities the levels connected by the microwave field suffer AC stark shift resulting in increased  $|\chi_p^{(2)}|$  values away from resonance. This effect in the frequency domain translates to the ringing effect in the time domain.

To see the effect of Doppler broadening on the group delay of the generated probe pulse we have done a Doppler averaging of the  $\chi_p^{(2)}$  susceptibility profile. We incorporate Doppler broadening by defining the Doppler shifted detunings as

$$\Delta_c(v) = \Delta_c - \omega_{12}v/c, \quad \Delta_p(v) = \Delta_p - \omega_{13}v/c, \quad (27)$$

where  $v$  is the velocity of atom. We average  $\chi_p^{(2)}$  using the Maxwell-Boltzmann velocity distribution for room temperature  $T=300 \text{ K}$ . This procedure leads to the Doppler averaged  $t^{(2)}$  using Eqs. (18) and (22) and is plotted in Fig. 9. It is clear from this figure that even with room temperature atoms a microwave-intensity change acts as an effective knob to convert a delayed pulse to an advanced pulse. However, this change happens at a higher microwave intensity. For a

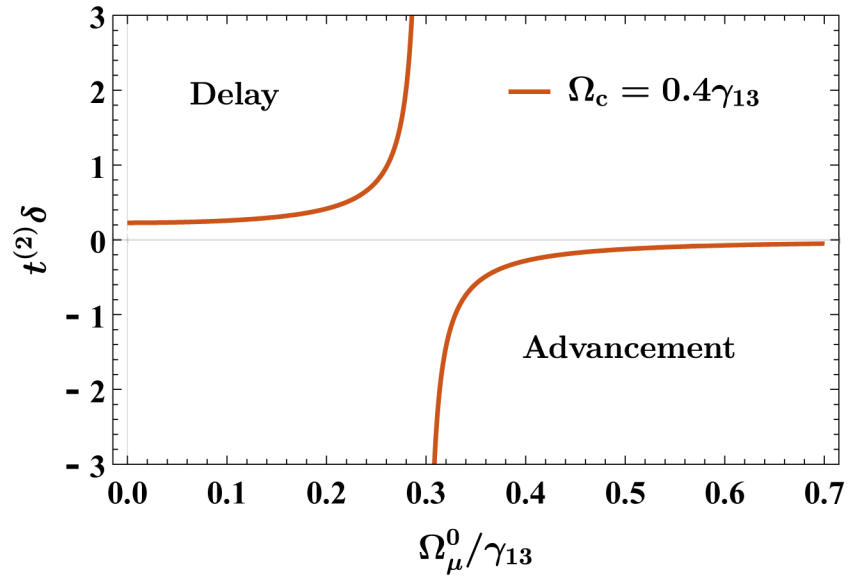


**Fig. 6.** Group delay due to generation phase as function of the microwave amplitude, for  $\delta = 0.3 \times 10^6$  Hz,  $N = 10^6$  cm $^{-3}$  and  $\gamma_{13} = 5\pi \times 10^6$  rad/s.

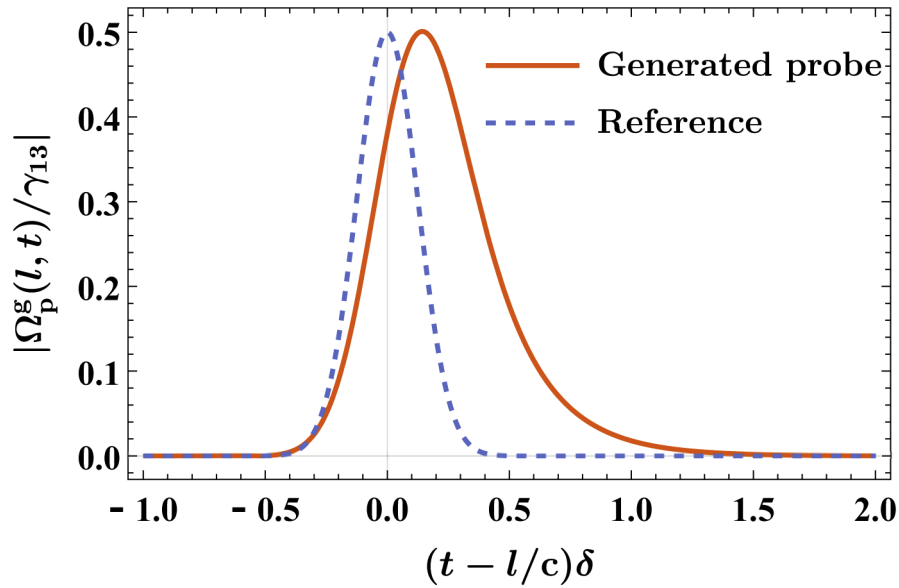


**Fig. 7.** Delay of  $0.5 \mu\text{s}$  observed in the generated probe with respect to the reference, for  $\Omega_\mu^0 = 0.004\gamma_{13}$ ,  $\Omega_c = 0.4\gamma_{13}$ ,  $\delta = 0.3 \times 10^6$  Hz,  $\gamma_{13} = 5\pi \times 10^6$  rad/s,  $N = 10^6$  cm $^{-3}$  and  $l = 1$  cm. The mean number of photon in the generated probe is 1.24. The generated probe has been scaled by a factor of 10416. The parameters of the reference are  $\Omega_r^0 = 0.5\gamma_{13}$  and  $\sigma = 2.4 \times 10^6$  Hz.

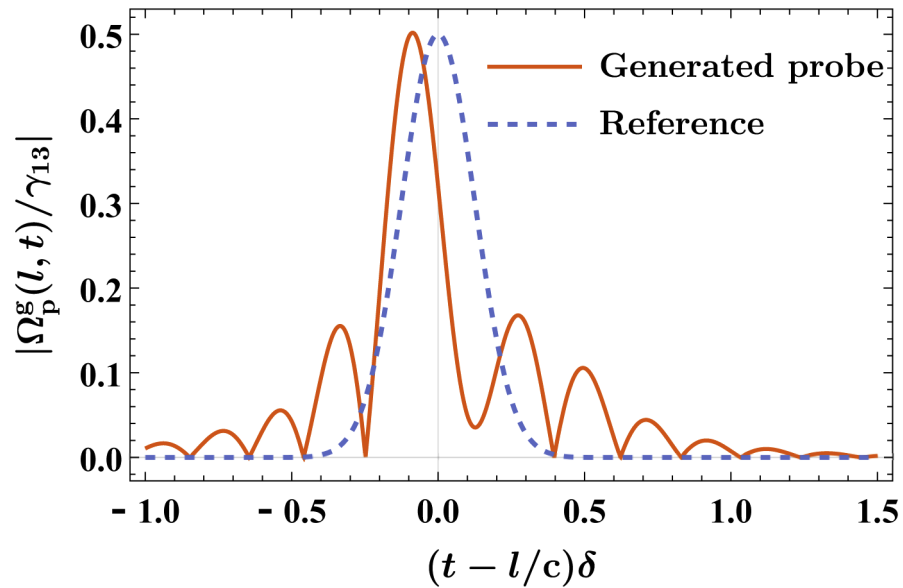


**Fig. 8.** Advancement of  $0.3 \mu\text{s}$  observed in the generated probe with respect to the reference, for  $\Omega_\mu^0 = 2.4\gamma_{13}$ ,  $\Omega_c = 0.4\gamma_{13}$ ,  $\delta = 0.3 \times 10^6 \text{ Hz}$ ,  $\gamma_{13} = 5\pi \times 10^6 \text{ rad/s}$ ,  $\mathcal{N} = 10^6 \text{ cm}^{-3}$  and  $l = 100 \mu\text{m}$ . The mean number of photon in the generated probe is 1.29. The generated probe has been scaled by a factor of 75757. The parameters of the reference are  $\Omega_r^0 = 0.5\gamma_{13}$  and  $\sigma = 2.4 \times 10^6 \text{ Hz}$ .

temperature of  $100^\circ\text{C}$  the microwave amplitude required to change from delay to advancement is about 6 % more than what is required at room temperature.

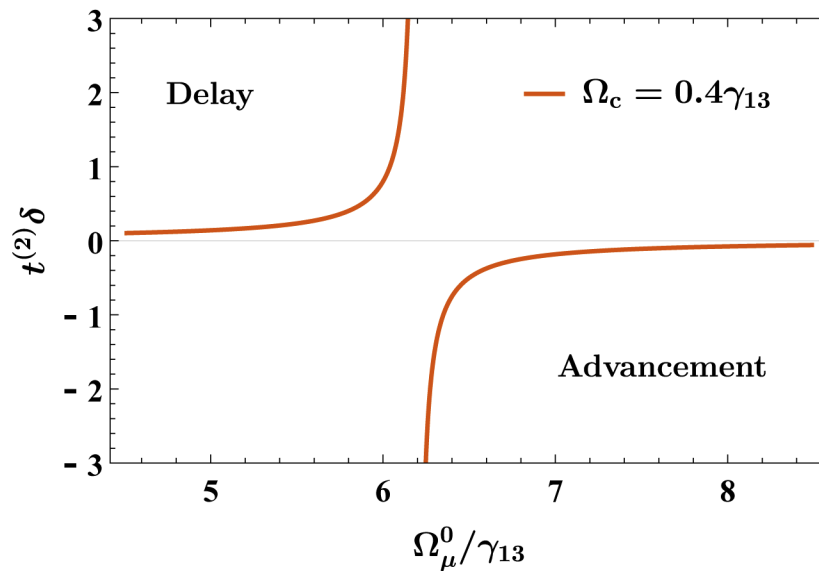


**Fig. 9.** Doppler averaged group delay due to generation phase as a function of microwave amplitude, for  $\gamma_{23} = 0.4\gamma_{13}$ ,  $T=300 \text{ K}$ ,  $\delta = 0.3 \times 10^6 \text{ Hz}$  and  $\gamma_{13} = 5\pi \times 10^6 \text{ rad/s}$ .

The repetition rate of the on-demand pulse with the ability to delay or advance the peak depends on the bandwidth of the near-linear region around  $\Delta_p = 0$  in Fig. 5. From this figure it is clear that the bandwidth is of the order of a few MHz for our parameters and so the repetition rate of our generation also would be in the order of a few MHz.

Experimental realization of generation and group delay control of a few photon pulse described above can be achieved. Generation of probe optical field with  $^{85}\text{Rb}$  atoms from a sum frequency process between the coupling and microwave fields has already been realized [34].

In order to show that the delay or advancement of the generated pulse is independent of number density or length of the cell, the number density in a vapour cell could be varied by changing the temperature or by using identical cells of varying vapour density or cells with varying physical dimensions.

#### 4. Conclusion

A scheme for on-demand generation of optical pulses and control of their group delay using a hybrid second order-nonlinearity in an atomic  $\Delta$  system is presented. An unexplored regime of manipulating group delay arising from the initial phase of the generated pulse is presented. We rigorously establish that this leads to density-independent group delays. We show that the generated pulse can be delayed or advanced through change in intensity of the input microwave field and discuss in detail the average photon number and temporal shape of the generated pulse. Thus, our scheme can be exploited to generate and control group delay of optical pulses with few photons using ultra-dilute samples with small spatial dimensions. These results open a way for producing and manipulating group delays with microscopic atomic systems that can be integrated in scalable platforms. All the above features in combination with our hybrid nonlinearity will have a definitive impact in introducing controllable delays in both classical and quantum information processing channels which use both microwave and optical fields.

**Disclosures.** The authors declare no conflicts of interest.

**Data availability.** Since this work is a theoretical proposal, no data were generated or analyzed in the presented research.

#### References

1. C. J. Chunnillall, I. P. Degiovanni, S. Kück, I. Müller, and A. G. Sinclair, "Metrology of single-photon sources and detectors: a review," *Opt. Eng.* **53**(8), 081910 (2014).
2. L. Schweickert, K. D. Jöns, K. D. Zeuner, S. F. Covre da Silva, H. Huang, T. Lettner, M. Reindl, J. Zichi, R. Trotta, A. Rastelli, and V. Zwillier, "On-demand generation of background-free single photons from a solid-state source," *Appl. Phys. Lett.* **112**(9), 093106 (2018).
3. X. Ding, Y. He, Z.-C. Duan, N. Gregersen, M.-C. Chen, S. Unsleber, S. Maier, C. Schneider, M. Kamp, S. Höfling, C.-Y. Lu, and J.-W. Pan, "On-demand single photons with high extraction efficiency and near-unity indistinguishability from a resonantly driven quantum dot in a micropillar," *Phys. Rev. Lett.* **116**(2), 020401 (2016).
4. Z. Peng, S. De Graaf, J. S. Tsai, and O. Astafiev, "Tuneable on-demand single-photon source in the microwave range," *Nat. Commun.* **7**(1), 12588 (2016).
5. J.-Y. Hu, B. Yu, M.-Y. Jing, L.-T. Xiao, S.-T. Jia, G.-Q. Qin, and G.-L. Long, "Experimental quantum secure direct communication with single photons," *Light: Sci. Appl.* **5**(9), e16144 (2016).
6. A. Jain, P. V. Sakhiya, and R. K. Bahl, "Design and development of weak coherent pulse source for quantum key distribution system," in *2020 IEEE International Conference on Electronics, Computing and Communication Technologies (CONECCT)*, (2020), pp. 1–5.
7. J.-i. Yoshikawa, K. Makino, S. Kurata, P. van Loock, and A. Furusawa, "Creation, storage, and on-demand release of optical quantum states with a negative wigner function," *Phys. Rev. X* **3**(4), 041028 (2013).
8. I. Aharonovich, D. Englund, and M. Toth, "Solid-state single-photon emitters," *Nat. Photonics* **10**(10), 631–641 (2016).
9. M. Lukin and A. Imamoglu, "Controlling photons using electromagnetically induced transparency," *Nature* **413**(6853), 273–276 (2001).
10. M. D. Eisaman, A. André, F. Massou, M. Fleischhauer, A. S. Zibrov, and M. D. Lukin, "Electromagnetically induced transparency with tunable single-photon pulses," *Nature* **438**(7069), 837–841 (2005).
11. A. Kasapi, M. Jain, G. Y. Yin, and S. E. Harris, "Electromagnetically induced transparency: Propagation dynamics," *Phys. Rev. Lett.* **74**(13), 2447–2450 (1995).

12. O. Schmidt, R. Wynand, Z. Hussein, and D. Meschede, "Steep dispersion and group velocity below  $c/3000$  in coherent population trapping," *Phys. Rev. A* **53**(1), R27–R30 (1996).
13. L. V. Hau, S. E. Harris, Z. Dutton, and C. H. Behroozi, "Light speed reduction to 17 metres per second in an ultracold atomic gas," *Nature* **397**(6720), 594–598 (1999).
14. M. M. Kash, V. A. Sautenkov, A. S. Zibrov, L. Hollberg, G. R. Welch, M. D. Lukin, Y. Rostovtsev, E. S. Fry, and M. O. Scully, "Ultraslow group velocity and enhanced nonlinear optical effects in a coherently driven hot atomic gas," *Phys. Rev. Lett.* **82**(26), 5229–5232 (1999).
15. D. Budker, D. F. Kimball, S. M. Rochester, and V. V. Yashchuk, "Nonlinear magneto-optics and reduced group velocity of light in atomic vapor with slow ground state relaxation," *Phys. Rev. Lett.* **83**(9), 1767–1770 (1999).
16. L. J. Wang, A. Kuzmich, and A. Dogariu, "Gain-assisted superluminal light propagation," *Nature* **406**(6793), 277–279 (2000).
17. A. Dogariu, A. Kuzmich, and L. J. Wang, "Transparent anomalous dispersion and superluminal light-pulse propagation at a negative group velocity," *Phys. Rev. A* **63**(5), 053806 (2001).
18. H. Tanaka, H. Niwa, K. Hayami, S. Furue, K. Nakayama, T. Kohmoto, M. Kunitomo, and Y. Fukuda, "Propagation of optical pulses in a resonantly absorbing medium: Observation of negative velocity in rb vapor," *Phys. Rev. A* **68**(5), 053801 (2003).
19. K. Kim, H. S. Moon, C. Lee, S. K. Kim, and J. B. Kim, "Observation of arbitrary group velocities of light from superluminal to subluminal on a single atomic transition line," *Phys. Rev. A* **68**(1), 013810 (2003).
20. G. S. Agarwal, T. N. Dey, and S. Menon, "Knob for changing light propagation from subluminal to superluminal," *Phys. Rev. A* **64**(5), 053809 (2001).
21. D. Bortman-Arbiv, A. D. Wilson-Gordon, and H. Friedmann, "Phase control of group velocity: from subluminal to superluminal light propagation," *Phys. Rev. A* **63**(4), 043818 (2001).
22. A. D. Wilson-Gordon and H. Friedmann, "Positive and negative dispersion in a three-level  $\lambda$  system driven by a single pump," *J. Mod. Opt.* **49**(1-2), 125–139 (2002).
23. M. Sahrar, H. Tajalli, K. T. Kapale, and M. S. Zubairy, "Tunable phase control for subluminal to superluminal light propagation," *Phys. Rev. A* **70**(2), 023813 (2004).
24. H. Sun, H. Guo, Y. Bai, D. Han, S. Fan, and X. Chen, "Light propagation from subluminal to superluminal in a three-level  $\lambda$ -type system," *Phys. Lett. A* **335**(1), 68–75 (2005).
25. S. Davuluri and Y. V. Rostovtsev, "Switching between superluminal to subluminal velocities and tunable slow light in a four level atomic system," *J. Phys.: Conf. Ser.* **414**, 012005 (2013).
26. V. Boyer, C. F. McCormick, E. Arimondo, and P. D. Lett, "Ultraslow propagation of matched pulses by four-wave mixing in an atomic vapor," *Phys. Rev. Lett.* **99**(14), 143601 (2007).
27. R. T. Glasser, U. Vogl, and P. D. Lett, "Stimulated generation of superluminal light pulses via four-wave mixing," *Phys. Rev. Lett.* **108**(17), 173902 (2012).
28. J. Jing, Z. Zhou, C. Liu, Z. Qin, Y. Fang, J. Zhou, and W. Zhang, "Ultralow-light-level all-optical transistor in rubidium vapor," *Appl. Phys. Lett.* **104**(15), 151103 (2014).
29. A. B. Matsko, D. V. Strekalov, and L. Maleki, "On the dynamic range of optical delay lines based on coherent atomic media," *Opt. Express* **13**(6), 2210–2223 (2005).
30. E. Choi, J. Na, S. Y. Ryu, G. Mudhana, and B. H. Lee, "All-fiber variable optical delay line for applications in optical coherence tomography: feasibility study for a novel delay line," *Opt. Express* **13**(4), 1334–1345 (2005).
31. A. W. Elshaari, W. Pernice, K. Srinivasan, O. Benson, and V. Zwiller, "Hybrid integrated quantum photonic circuits," *Nat. Photonics* **14**(5), 285–298 (2020).
32. M. Manjappa, S. S. Undurti, A. Karigowda, A. Narayanan, and B. C. Sanders, "Effects of temperature and ground-state coherence decay on enhancement and amplification in a  $\Delta$  atomic system," *Phys. Rev. A* **90**(4), 043859 (2014).
33. S. Davuluri and Y. Rostovtsev, "Optical control of backward and forward microwave generation," *Phys. Rev. A* **88**(5), 053847 (2013).
34. K. V. Adwaith, A. Karigowda, C. Manwatkar, F. Bretenaker, and A. Narayanan, "Coherent microwave-to-optical conversion by three-wave mixing in a room temperature atomic system," *Opt. Lett.* **44**(1), 33–36 (2019).
35. R. W. Boyd, *Nonlinear Optics* (Academic, 2008), 3rd ed.